Insights of Tris(2-pyridylmethyl)amine as anti-tumor agent for osteosarcoma: experimental and in silico studies

Marcos V. Palmeira-Mello, Juliana Lima Souza, Anthuan Ferino Pérez, Amanda dos Santos Cavalcanti, Suzana Assad Kahn, Nady Passe-Coutrin, Idania Rodeiro Guerra, Antonio Doménech-Carbó, Ulises Javier Jauregui-Haza, Alessandra Mendonça Teles de Souza, et al.

Insights of Tris(2-pyridylmethyl)amine as anti-tumor agent for osteosarcoma: experimental and *in silico* studies

Marcos V. Palmeira-Mello[a,b], Juliana Lima Souza[c], Anthuan Ferino Pérez[d], Amanda dos Santos Cavalcanti[c], Suzana Assad Kahn[c], Nady Passe-Coutrin[e], Idania Rodeiro Guerra[f], Antonio Doménech-Carbó[g], Ulises Javier Jauregui-Haza[d,h], Alessandra Mendonça Teles de Souza[b], Mauricio Lanznaster[a], Gerardo Cebrián-Torrejón[a,e,†]

[a] *Instituto de Química, Universidade Federal Fluminense, Outeiro S. Joao Batista S/ N, 24020-141 Niterói, RJ, Brazil.*

[b] *Faculdade de Farmácia, Universidade Federal do Rio de Janeiro, 21941-590 Rio de Janeiro, RJ, Brazil.*

[c] *Instituto Nacional de Traumatologia e Ortopedia, Divisão de Pesquisa, Avenida Brasil, 500, São Cristóvão, 20940-070, Rio de Janeiro, RJ, Brazil.*

[d] *Instituto Superior de Ciencias y Tecnologías Aplicadas, Universidad de La Habana, Cuba.*

[e] *Departement de Chimie, Université des Antilles, Pointe-à-Pitre, Guadeloupe (FWI)*

[f] *Instituto de Ciencias del Mar, La Habana, Cuba.*

[g] *Departament de Química Analítica, Facultat de Química, Universitat de València, Dr. Moliner 50, 46100 Burjassot, Valencia, Spain.*

[h] *Instituto Tecnológico de Santo Domingo, Ave. Próceres 49, Los Jardines del Norte, 10602, Santo Domingo, República Dominicana.*

† *E-mail: gerardo.cebrian-torrejon@univ-antilles.fr*

Highlights

TPA presents antitumor activity against MG-63 and Saos-2 osteosarcoma cells.

DNA-interacting studies by cyclic voltammetry were performed.

Molecular docking studies were conducted for DNA and other biological targets.

Good pharmacokinetic and toxicological profile obtained via ADMET *in silico* analysis.

Abstract

Osteosarcoma (OS) is a malignant bone tumor and its occurrence is associated with high levels of microRNAs (miRNAs) and critical protein sinvolved on intracellular signaling pathways. Cisplatin and Doxorubicin are employed on chemotherapy, but their use cause side effects and contributes to multidrug resistance. Since several tripodal amines have been studied as anticancer agents, tris(2-pyridylmethyl)amine (TPA) was investigated against osteosarcoma cells. Here we show that TPA exhibits activity against MG-63 and Saos-2 cells. Cyclic voltammetry results indicate an interaction between TPA and dsDNA, denoted by blocking of the proton-assisted reduction of the 2-pyridylmethyl moiety in the presence of the biomolecule. Molecular docking studies indicate binding modes between TPA and DNA, as well as other crucial biological targets related to OS pathology. In addition, ADMET *in silico* prediction results suggest a good pharmacokinetic and toxicity profile for TPA.

1. Introduction

Osteosarcoma (OS) is an aggressive malignant bone tumor that occurs in children and young adults [1,2,3]. Currently, therapies involve surgical resection and combinational chemotherapy, in which cisplatin and doxorubicin can be used with or without methotrexate [4]. The response to this strategy is the strongest indicator of OS patients overall survival [5]. Several randomized studies have shown that combination of chemotherapy and surgery significantly improved the 5-year survival rates to 75% in patients with nonmetastatic OS and 25% in patients with metastatic disease [6,7,8,9]. Whereas cisplatin acts via covalent binding on the DNA, forming DNA-platinum adducts, doxorubicin acts via intercalation with base pairs of double helix 10 , 11]. Nonetheless, doxorubicin is efficiently exported out of cells, mediated via P glycoprotein (Pgp), which levels are increased in OS, contributing to the development of multidrug resistance [12].

In contrast to healthy tissues, OS is associated to increased amounts of microRNAs (miRNAs) [13,14] and proteins [15,16,17] involved on different signaling pathways. This condition plays an important role in the carcinogenesis process, also favoring the tumor survival and resistance. Therefore, these agents seem to be attractive targets to development of new anticancer drugs.

Several tripodal amines have been investigated as anticancer agents, alone or bounded to metal centers [18,19,20,21,22,23,24,25,26,27,28,29]. The family of tetradentate tripodal amines have a general structure consisting of a central donor atom of nitrogen attached to three independent arms, each one also containing at least one methylene group and a donor atom. These compounds can be synthesized using different methodologies, with the route of

choice generally guided by the nature of the donor atoms on the three arms [30]. Since survival of patients with OS is still low, the development of more active and safe anti-OS drugs is extremely needed. In this context, we report the anticancer activity of a tripodal amine named tris-(2-pyridylmethyl)amine (TPA) against MG-63 and Saos-2 osteosarcoma cells. DNA-interacting experiments by cyclic voltammetry, quantum chemical calculations, molecular docking and ADMET *in silico* studies were also performed.

2. Experimental

2.1. Chemistry

TPA was obtained via procedure previously described [22],and characterized by IR and ^{1}H NMR techniques (See Supplementary data, Figs. 1S and 2S).

2.2. Anticancer Activity

2.2.1. Cell Lines

Osteosarcoma cell lines, MG-63 and Saos-2, were purchased from the Cell Bank of Rio de Janeiro (BCRJ/UFRJ), and maintained at 37 ^{o}C / 5% CO_2 with culture medium DMEM (Dulbecco's Modified Eagle Medium) (Gibco), supplemented with 10% Fetal Bovine Serum (FBS, Gibco) and 1% antibiotic/antimycotic (0.5 mg/mL, Sigma-Aldrich).

2.2.2. MTT cytotoxicity assays

Osteosarcoma cells were cultured with DMEM-F12 medium supplemented with 10% FBS and 1% antibiotic/antimycotic (Sigma-Aldrich) in 96-well flat bottom plates for 24 h. Cells were then treated with 50, 100, 250 or 500 µM TPA or with the vehicle DMSO (Dimethyl Sulfoxide, Amresco) for 24 h. Viable cells were

quantified by the MTT cytotoxicity assay [31], and the cell viability was measured in a spectrophotometer (Glomax Multi Detection System, Promega, Madison, WI, USA) at each concentration as the ratio of absorbance at 560 nm, relative to vehicle-treated cells. Statistical analyses were accessed by comparison between compound versus vehicle for each concentration utilizing Unpaired T test and Kruskal-Wallis test followed by Dunn's multiple comparisons post-test. Results were expressed as average ± standard error for the three independent experiments.

2.3. Electrochemical Experiments

Eukaryotic double stranded deoxyribonucleic acid from *Rhagovelia plumbea* (dsDNA) was kindly donated by the laboratoire YSYEB from University of Antilles (Guadeloupe, France). Electrochemical experiments were performed at 298 ± 1K in a thermostated cell with CH I660 equipment. A typical three-electrode arrangement was used: a BAS MF2012 glassy carbon working electrode (GCE) (geometrical area 0.071 cm^2), a platinum wire auxiliary electrode and an Ag/AgCl (3 M NaCl) reference electrode. Experiments in aqueous media were performed in 0.10 M potassium phosphate buffer saline at pH 7.4 with and without DNA. The electrochemical analysis was performed on TPA films, deposited in the surface of the glassy carbon electrode using the methodology previously described [32,33]. An ethanol solution of TPA (10 µL, 1 mg/mL), previously ultrasonicated by 5 min, was added to the surface of electrode and the solvent was allowed to evaporate in air, resulting in a uniform fine coating of the TPA (L) adhered to the electrode. Paraffin-impregnated graphite electrodes (PIGEs) were also used for complementary experiments.

The lower end of the graphite electrode was gently rubbed over that spot of sample and cleaned with a tissue paper. Controlled potential cyclic voltametry experiments were performed at L-modified electrodes by applying constant potentials between –1.5 and +1.5 V and a 10 mV/s scan rate.

2.4. Molecular modeling and in silico ADMET studies

2.4.1. Quantum chemical calculations

Quantum chemical calculations were carried out using SPARTAN'10 program (Wavefunction Inc., Irvine, CA, 2000). In order to select the lowest energy conformation, TPA was subjected to conformational analysis using molecular mechanics calculations using water as a solvent ($MMFF_{aq}$). Then, the best conformer was submitted to a geometry optimization using PM6 method. Finally, the structural and electronic properties as Highest Occupied Molecular Orbital (HOMO) and Lowest Unoccupied Molecular Orbital (LUMO) energies and coefficient of distribution, and molecular electrostatic potential (MEPs) maps were calculated with DFT B3LYP/6-31G* basis set. The three-dimensional isosurfaces of MEPs at the van der Waals contact surface represent electrostatic potentials superimposed onto a surface of constant electron density (0.002 e/au^3) and generated at a range of –200 to +100 kcal/mol. These color-coded isosurface values provide an indication of the overall molecular size and location of negative (red) or positive (blue) electrostatic potentials.

2.4.2. Molecular Docking

In order to obtain better insights about the TPA activity, a molecular docking study was performed using two DNA targets (called DNA-1 and DNA-2, respectively), one miRNA (pre-miR21) and three proteins: Bcl2-associated at hanogene 3 (BAG-3), B-cell lymphoma extra-large (Bcl-$_X$L) and caspase-3. After removing all bound water molecules, the PDB2PQR server [34,35] was used to construct the all-atom model of the molecular targets employing AMBER force field [36]. The preparation for molecular docking simulations of both ligand and receptors were performed using AutoDockTools4 [37]. Gasteiger partial charges [38,39] were added for describing the charge distribution of all molecules and the Lamarckian Genetic Algorithm (LGA) [40]was employed for all docking calculations. Docking parameters were set to 0.35 Å as grid space and different points for all six targets (DNA-1, 90x90x82; DNA-2, 67x84x90; pre-miR21, 100x130x130; BAG-3, 125x160x125; BcL-$_X$L, 120x140x100; caspase-3, 250x231x248). A total of 100 LGA runs were performed for each ligand/receptor system. All docking calculations were carried out using Autdock 4.26 software package. The results of the most favorable free energy binding were selected. The exploration of the ligand interactions with the proposed targets was performed using LigPlot+ software [41,42].

2.4.3. ADMET in silico evaluation

Pharmacokinetic and toxicology prediction for TPA and doxorubicin were performed using ADMET Predictor 9.5™ (Simulations Plus Inc., Lancaster, CA, USA), an approach based on the degree of concordance among the individual QSAR networks in an ensemble model. The compounds were submitted to analysis using ADMET Risk. Additionally, specific toxicity

parameters such as mutagenicity, hepatotoxicity and reproductive toxicity were evaluated. Mutagenicity was predicted based on Ames Test. The elevation of important biomarkers as Alkaline Phosphatase (ALP), Serum Aspartate Transaminase (AST), Serum Alanine Transaminae (ALT), Gamma-Glutamyltransferase (GGT) and Lactate Dehydrogenase (LDH) enzymes were investigated on hepatotoxicity prediction.

3. Results

The tripodal amine TPA was synthesized in two steps (Scheme 1). First, the reaction between the amine and aldehyde moieties produced the imine compound, which was reduced by catalytic hydrogenation. Thus, the tripodal amine compound was obtained via nucleophilic substitution between the secondary amine and 2-(chloromethyl)pyridine (35% yield). TPA was characterized by spectroscopic techniques. Infrared spectra shows characteristic bands at 1586–1433 cm^{-1} typical of C=C and C=N bonds. Thus, bands around 3010 cm^{-1} were assigned to C–H group. ^{1}H NMR spectrum of 1 measured in DMSO-d_6 confirms the molecular structure of **1**. The pyridine Hα was observed at 8.74 (d) ppm (3 H). Additional aromatic hydrogens were found at 8.15 (t), 7.74 (d) and 7.64 (t) ppm (9 H). Finally, the aliphatic hydrogens were found at 4.35 (s) ppm (6 H) (Figs. 1S and 2S).

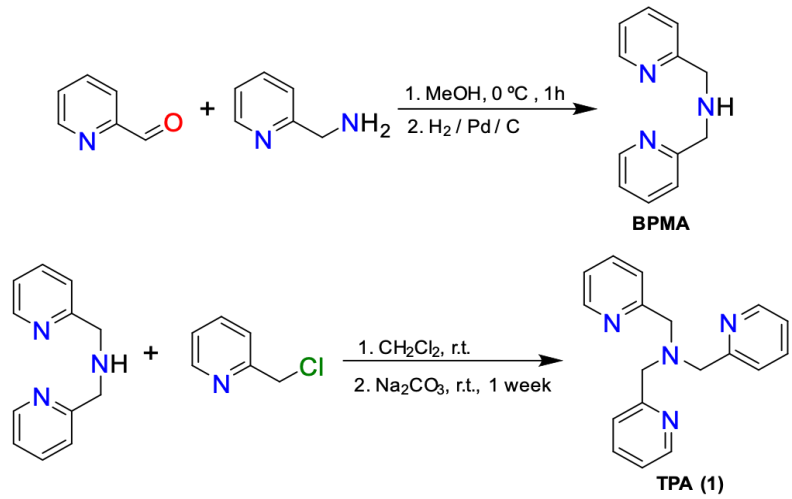

Scheme 1. Synthesis of tris-(2-pyridylmethyl)amine (TPA).

MTT assays were performed to determine the effect of TPA on well characterized human osteosarcoma cells[43] [44].The results showed that TPA decreased the viability ofMG-63 and Saos-2 cell lines, exhibiting IC_{50} values of 50 and 91 µM, respectively (Fig. 1).

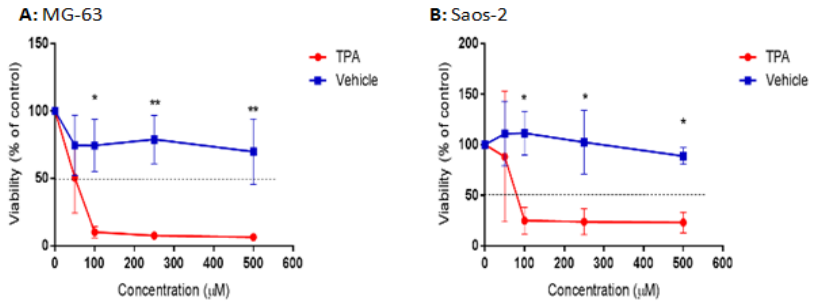

Fig. 1. The effects of TPA in (A) MG-63 and (B) Saos-2 cells treated with 50, 100, 250 or 500 µM TPA diluted in DMSO (vehicle) for 24 h. Points represent the average of three individual experiments. Kruskal-Wallis and Dunn's multiple comparisons test.**p<0.001; *p<0.05.*

Since DNA is an important target related to cancer cells, the interaction between TPA and dsDNA was studied by cyclic voltammetry. A TPA-modified electrode was used in contact with dsDNA solutions, in phosphate buffer at biological pH value, following the voltammetry of immobilized particles [45,46,47,48]. This methodology was previously employed in monitoring the

performance of drugs with antimalarial properties and screening of DNA [32,49]. The cyclic voltammogram results recorded at a TPA-modified GCE in contact with air-saturated 0.10 M potassium phosphate buffer saline at pH 7.4are presented in Fig. 2. Voltammogram shows cathodic waves at –1.1 (C1) and –1.5 V (C2), preceded by a weak signal at -0.6 V, and a prominent anodic signal at the extreme of tested positive potentials ca. 1.5 V (A1). The weak cathodic shoulder at –0.6 V can be assigned to the reduction of dissolved oxygen as judged by blank experiments at unmodified GCE. Under the same conditions, dsDNA solutions remain electrochemically silent at unmodified GCE. The large anodic current A1 at 1.5 V can be attributed to the oxidative degradation of TPA starting from the formation of radicals on the aromatic rings whereas the cathodic wave at –1.5 V (process C2) can be assigned to the catalytic proton reduction preceded by protonation of the central nitrogen. In turn, the cathodic peak C1 at –1.1 V can be attributed to the solid state reduction of TPA mediated by proton insertion. This process can be described as below:

$$\{TPA\}_{solid} + 2H^{+}_{aq} + 2e^{-} \rightarrow \{TPAH_2\}_{solid} \quad (1)$$

Cyclic voltammogram of a saturated dsDNA solution in air-saturated 0.10 M potassium phosphate buffer saline at pH 7.4 recorded at a TPA-modified GCE are show in Fig. 3. Remarkably, the cathodic signal C1 vanishes whereas the wave C2 remains essentially unchanged and the intensity of the anodic current A1 diminishes. The vanishement of signal C1 can unambiguously be attributed to the coordination between TPA and dsDNA which blocks the proton-assisted reduction of the 2-pyridylmethyl moiety. Electrochemical data at TPA-modified electrodes indicate the existence of a significant interaction

between TPA and dsDNA as denoted by the blocking of the proton-assisted reduction of the 2-pyridylmethyl units in the presence of dsDNA. This information is confirmed by the docking study of interaction between TPA and DNA.

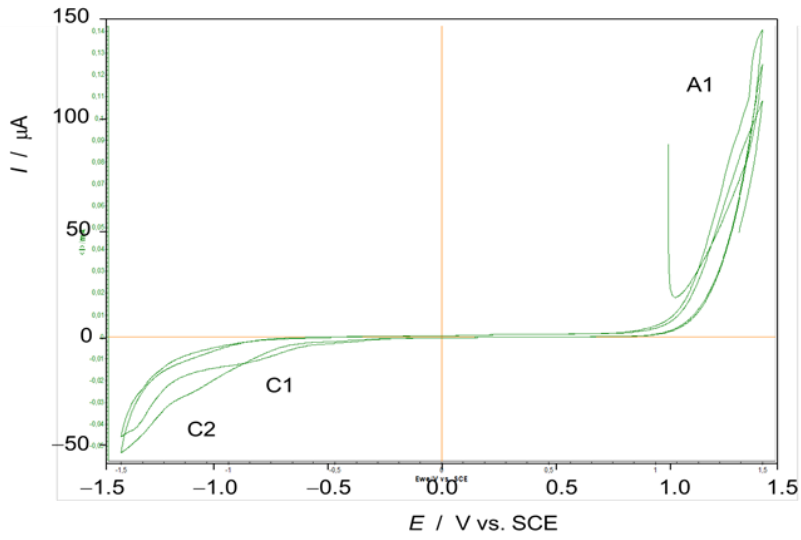

Fig. 2. Cyclic voltammogram of a TPA-modified GCE in contact with air-saturated solution in 0.10 M potassium phosphate buffer saline at pH 7.4. Potential scan rate 20 mV s^{-1}

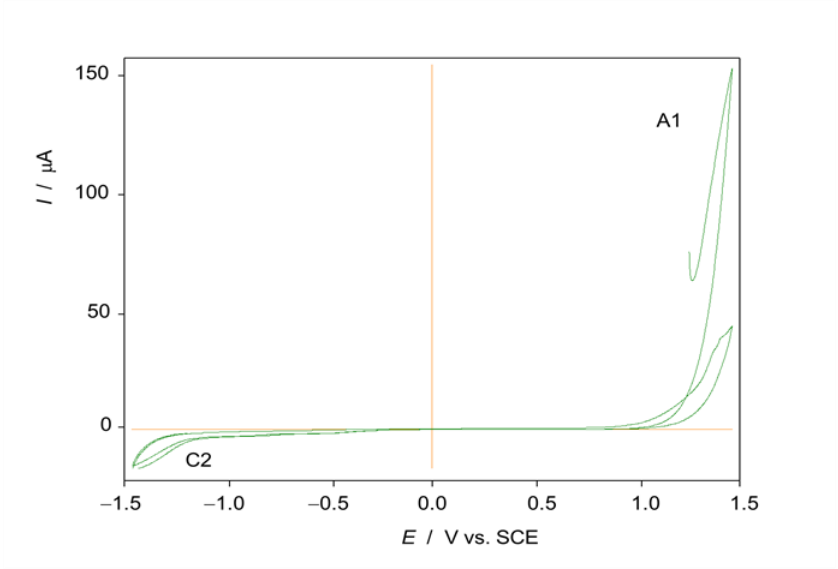

Fig. 3. Cyclic voltammogram of a TPA-modified GCE in contact with air-saturated saturated dsDNA solution in 0.10 M potassium phosphate buffer saline at pH 7.4. Potential scan rate 20 mV s^{-1}.

Quantum chemical calculations for TPA were also performed to gain better insight of its electronic properties. In this direction, some molecular descriptors were obtained, such as HOMO (Highest Occupied Molecular Orbital) and LUMO (Lowest Unoccupied Molecular Orbital) energy values and orbital coefficient and molecular electrostatic potential (MEPs) maps.These descriptors are employed in SAR/SPR studies and can be used to obtain a correlation with biological activities or properties exhibited by different compounds [50,51,52]. In TPA molecule, the HOMO is concentrated on tertiary nitrogen atom, whereas LUMO show a π density localized over the pyridine rings (Fig. 4).Higher E_{HOMO} values are observed for compounds with greater tendency to donate electrons, whereas the tendency to accept electrons are related to lower E_{LUMO} values. Since that TPA have lower E_{HOMO} (–6.02 eV) and E_{LUMO} (–0.71 eV), our results suggest its interaction with electron rich bases of DNA. Moreover, it's suggested a lower reactivity for TPA due to higher HOMO-LUMO gap (ΔE = 5.31 eV).

Further, the molecular electrostatic potential (MEP) map was obtained in attempt to investigate alterations on charge distribution over TPA. As expected, TPA presents deficient electronic areas due to the presence of pyridine moieties (Fig. 4). Moreover, negative electrostatic potentials are over the pyridine nitrogen atoms, whereas the positive and neutral electrostatic potentials are over the nitrogen amine atom and delocalized over the aromatic rings. Since this approach can be used to investigate the possibility of interaction between TPA and biological targets via charge complementarity, our results reinforce its electron-accepting property, which is related to its high electrophilic character.

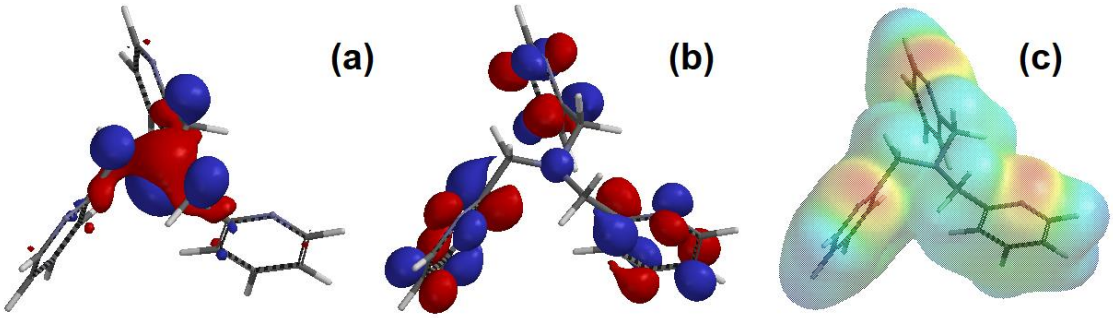

Fig. 4. Distribution coefficient of (a) Higher Occupied Molecular Orbital, (b) Lowest Unoccupied Molecular Orbital, and (c) Molecular Electrostatic Potential Map (MEP) for TPA. The color-coded isosurface values provide an indication of the overall molecular size and location of negative (red) or positive (blue) electrostatic potentials(range –200 to +100 kcal/mol).

Thus, a molecular docking approach was applied to obtain better insights about anti-osteosarcoma activity of TPA. These studies were performed of TPA with DNAs (PDB: 1BNA and 1ZEW) [53,54],a miRNA (pre-miR21,PDB: 5UZT) [55] and three proteins, BAG-3(PDB: 1UK5) [56], Bcl-$_X$L (PDB: 1R2D) [57] and caspase-3 (PDB: 3DEI) [58], since these proteins present key roles on OS pathology [13,14,15,16,17]. Molecular docking was carried out using Autodock 4.26 software. After the preparation of ligand and receptors, the parameters were set and 100 LGA runs were performed. The most favorable free energy binding with all six targets studied were obtained in the range –6.02 to –7.80 kcal/mol. These values are very similar and the differences negligible since they are in the range of Autodock's score function standard error [59].

The complexes formed between TPA and these targets were investigated (Fig. 5).The results showed that the DNA-binding of TPA takes place via minor groove interactions where the compound mostly interacts with adenine and thymine basis of this region via hydrophobic contacts. Moreover, a hydrogen bond was observed between TPA and cytosine with distance of 3.03 Å. Although most DNA-cleavage mechanisms are related to the presence of metal ions, these results suggest that the DNA-binding properties of TPA might

interfere with its interaction with proteins or expression factors disrupting the cellular cycle or other process essential to cell survival.

Besides DNA, miRNAs also play an important function on cancer process. It has been suggested that this agents can be employed on clinical applications, helping on early diagnostics of OS [14]. TPA molecule interacts with both 5' and 3' strands of miRNA molecule through van der Walls interactions; hydrogen bonds were also observed between TPA and guanine and cytosine, with distance of 2.80 and 3.21 Å, respectively. In this case, TPA binding to pre-microRNA-21 occurs at the apical portion of the stem-loop which is suggested to have an inhibitory effect [55]. This would interfere with the biogenesis of miRNAs reducing mature miRNA levels in cancer cells where they are over-expressed.

OS cells express high levels of proteins that are crucial for different biological processes. Moreover, these compounds play essential functions related to cell death, and mediate the regulation of different pathways on OS therapy, being key targets on drug discovery and development [15,16,17]. The interaction between TPA and BAG3 occurs with the first of the three α-helices of protein, which is also reported to mediate BAG3 association with serine-threonine kinase Raf-1 [60]. Molecules with anti-proliferative activity across cancer cells had been reported as inhibitors of BAG3 protein-protein interaction with the Heat shock protein 70 (Hsp70) [61]. It should be noticed that this BAG3-Hsp70 interaction occurs through α_2- and α_3-helices and in consequence TPA binding to BAG3 at α_1-helix should not affect the binding of those proteins unless it induced some conformational changes in BAG3 molecule. Regarding to Bcl-X_L, the TPA interaction did not occur directly in the binding pocket

reported for its inhibitors [62], and hydrogen bonds are observed between the nitrogen atoms of pyridine and Lys20. Nevertheless, as it is interacting with the α-helix with a key role in the binding between Bcl-X_L and pro-apoptotic members of Bcl-2 family it could cause conformational changes preventing the anti-apoptotic function of this protein. In the case of caspase-3, the interaction with TPA did not take place in the reported binding site of the inhibitors of this protein [58], and hydrogen bonds are also observed between TPA and Glu248 and Phe250. As mentioned, the majority of these TPA-protein complexes interactions has a hydrophobic nature and takes place between the aromatic carbons of TPA and the different aminoacids in the binding sites. Since docking results suggest several possible targets for TPA and differences between experimental and computational results are expected, further studies are necessary to confirm their interaction, improving our findings reported here.

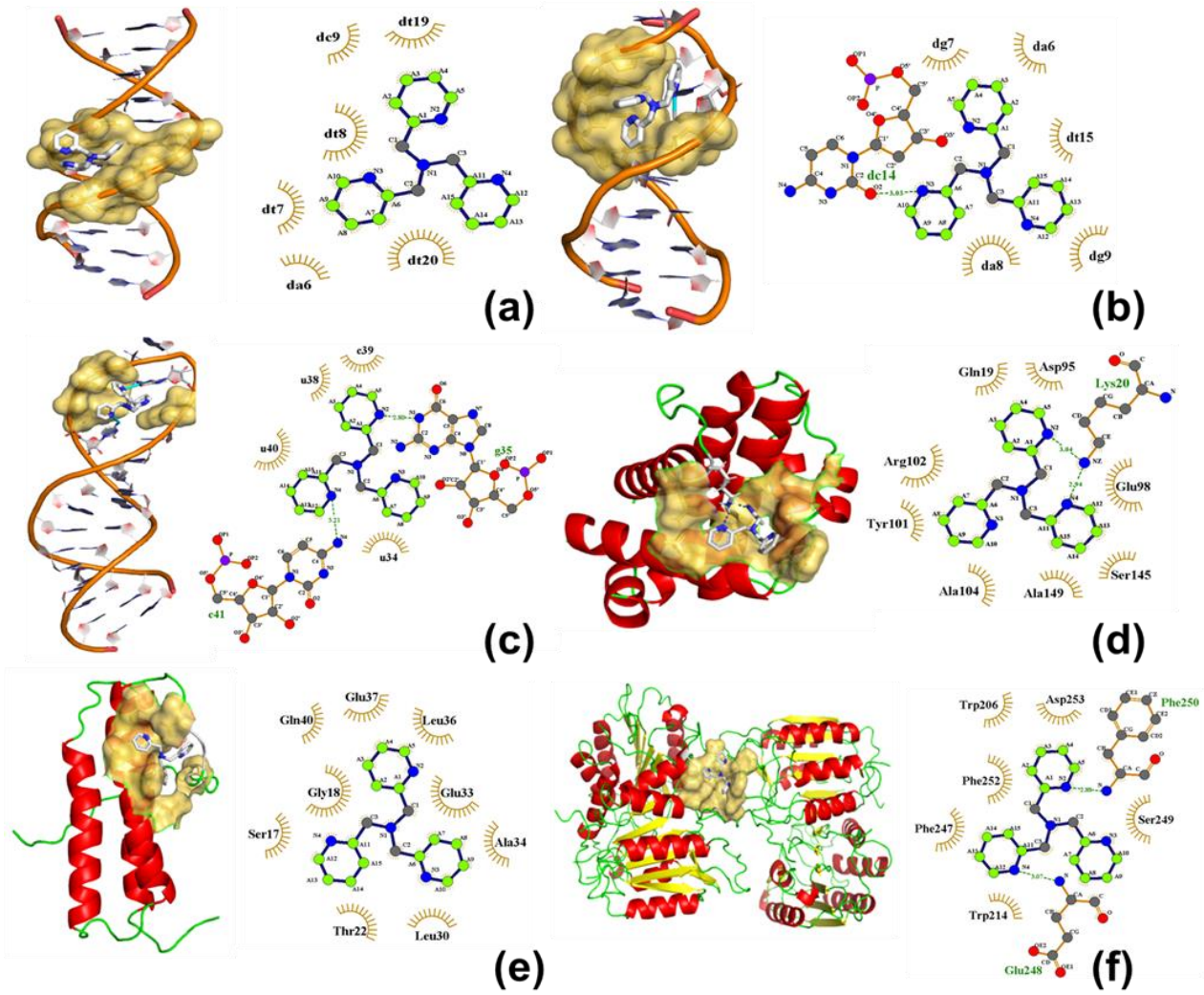

Fig. 5. Docking views of of TPA with (a) DNA-1, (b) DNA-2, (c) pre-miR21, (d) Bcl2-associated at hanogene 3 (BAG3), (e) Bcl-X_L, and (f) caspase-3.Hydrogen atoms are omitted for clarity. Hydrophobic interactions are shown as yellow lines around the nucleotide or residue name. H-bonds show the nucleotide or residue structure and a green dashed line linking interacting atoms.

Finally, we evaluated pharmacokinetic and toxicity properties of TPA using ADMET Predictor 9.5™ (Simulations Plus Inc., Lancaster, CA, USA). Our ADMET *in silico* prediction showed that TPA presented good bioavailability based on the Lipinski's Rule of 5 (Table 1) [63]. In addition, pharmacokinetics (Absorption, Distribution, Metabolism, and Excretion) and Toxicity parameters of TPA were compiled in the ADMET Risk, which showed a value of 1.93. ADMET risk provides a range between 0-24. These values indicate the number of potential ADMET risk factors that a compound might possess. It is interesting to

highlight that ADMET risk obtained for TPA is 3.6-fold lower than doxorubicin, which also violates parameters of the Lipinski's rule, except for lipophilicity (Table 1). Specific toxicological parameters such as mutagenicity, hepatotoxicity and reproductive toxicity were also predicted. Since that toxicity is a serious effect observed from doxorubicin administration, the analysis suggests that TPA would present lower toxicity problems than this antitumor drug [11].

Table 1. Parameters of oral bioavailability evaluated according Lipinski's Rule of 5, ADMET risk and specific toxicological parameters predicted for TPA and doxorubicin.

	TPA	Doxorubicin
MW (g/mol)	290.37	543.53
LogP	1.84	0.49
HBD	0	6
HBA	4	12
ADMET Risk	1.93	7.00
Hepatotoxicity	NO	NO
Mutagenicity	NO	YES
Reproductive toxicity	YES	YES

Conclusions

Experimental and *in silico* studies were performed to investigate the role of TPA as an anti-tumor agent against osteosarcoma. TPA reduced the viability of MG-63 and Saos-2 OS cells, suggesting its promising antitumor profile. Cyclic voltammogram recorded of a TPA-modified electrodes in presence of dsDNA indicates a significant interaction between these species. Quantum chemical investigation reveals a lower E_{LUMO} and reinforce the electrophilic character for TPA. Molecular docking studies indicate that interactions in all studied TPA/Target systems are composed by van der Walls and hydrophobic contacts, as well important hydrogen bonds with different nucleotides. Finally,

pharmacokinetic and toxicology predictions suggest that this compound might have oral administration. All data results pointed out TPA as a good skeleton for the design of antitumor drugs. Since all the biological targets studied can be considered, further investigations are necessary to confirm their interaction and the anti-osteosarcoma profile of TPA.

Acknowledgments

This work was supported by the Coordenação de Aperfeiçoamento de Pessoal de Nível Superior - Brazil (CAPES) - Finance Code 001. M. The authors thank to LAME (Laboratório Multiusuário de Espectroscopia) and LaReMN (Laboratório Multiusuário de Ressonância Magnética Nuclear) of Universidade Federal Fluminense, and INTO (Instituto Nacional de Traumatologia e Ortopedia) for the use of their facilities. Thanks are due to Prof. Olivier Gros from the laboratoire YSYEB (University of Antilles) for the kind donation of dsDNA.

Appendix A. Supplementary data

Supplementary data associated to this article can be found online at

References

[1] L. Mirabello, R.J. Troisi and S.A. Savage,Osteosarcoma incidence and survival rates from 1973 to 2004: data from the Surveillance, Epidemiology, and End Results Program. *Cancer.*115 (2009) 1531-1543, https://doi.org/10.1002/cncr.24121.

[2] D.M. Gianferante, L. Mirabello, S.A. Savage, Germline and somatic genetics of osteosarcoma - connecting aetiology, biology and therapy, *Nat Rev Endrocrinol*. 13 (2017) 480-491, https://doi.org/10.1038/nrendo.2017.16.

[3]L. Mirabello, R.J. Troisi and C.A. Savage,International osteosarcoma incidence patterns in children and adolescents, middle ages and elderly persons,*Int J Cancer.*125 (2009) 229-234, https://doi.org/10.1002/ijc.24320.

[4] A.S. Cavalcanti, W. Meohas, G.O. Ribeiro, A.C.S. Lopes, S. Ghloamin, M. Razavi, T.H.K. Brunswick, A. Avan, J.A.M. Guimarães, M.E.L. Duarte, S.A. Kahn, Patient-derived osteosarcoma cells are resistant to methotrexate. *PLoS One*. 12 (2017) e0184891,https://doi.org/10.1371/journal.pone.0184891.

[5]M. Collins, M. Wilhelm, R. Conyers, A. Herschtal, J. Whelan, S. Bielack, L. Kager, T. Kühne, M. Sydes, H. Gelderblom, S. Ferrari, P. Picci, S. Smeland, M. Eriksson, A.S. Petrilli, A. Bleyer, D.M. Thomas, Benefits and adverse events in younger versus older patients receiving neoadjuvant chemotherapy for osteosarcoma: findings from a meta-analysis. *J Clin Oncol.*31 (2013) 2303-2312,https://doi.org/10.1200/JCO.2012.43.8598.

[6]N. Jaffe, Historical perspective on the introduction and use of chemotherapy for the treatment of osteosarcoma. *Adv Exp Med Biol.*804 (2014) 1-30, https://doi.org/10.1007/978-3-319-04843-7_1.

[7]S. Bielack, H. Jurgens, G. Jundt, M. Kevric, T. Kühne, P. Reichardt, A. Zoubek, M. Werner, W. Winkelmann, R. Kotz, Osteosarcoma: the COSS experience.*Cancer Treat Res.*152 (2009) 289-308,https://doi.org/10.1007/978-1-4419-0284-9_15.

[8]X. Li, A.O Ashana, V.M. Moretti, R.D. Lackman, The relation of tumour necrosis and survival in patients with osteosarcoma,*Int Orthop.*35 (2011) 1847-1853, https://doi.org/10.1007/s00264-011-1209-7.

[9]J.H. Schwab, D.S. Springfield, K.A. Raskin, H.J. Mankin, F.J. Hornicek, What's new in primary malignant musculoskeletal tumors. *J Bone Joint Surg Am.* 95 (2013) 2240-2246, https://doi.org/10.2106/jbjs.16.00996.

[10]S. Dasari, P.B. Tchounwou, Cisplatin in cancer therapy: molecular mechanisms of action. *Eur J Pharmacol*. 0 (2014) 364-378, https://doi.org/10.1016/j.ejphar.2014.07.025.

[11] O. Tacara, P. Sriamornsak, C.R. Dass, Doxorubicin: an update on anticancer molecular action, toxicity and novel drug delivery systems. *J Pharm Pharmacol*65 (2013) 157-170,https://doi.org/10.1111/j.2042-7158.2012.01567.x.

[12]N. Baldini, K. Scotlandi, G. Barbanti-Bròdano, M.C. Manara, D. Maurici, G. Bacci, F. Bertoni, P. Picci, S. Sottili, M. Campanacci, M. Serra, Expression of P-Glycoprotein in High-Grade Osteosarcomas in Relation to Clinical Outcome. N *Engl J Med.*333 (1995) 1380-1385,https://doi.org/10.1056/NEJM199511233332103.

[13]Y.-H. Feng, C.-J. Tsao, Emerging role of microRNA-21 in cancer. *Biom Reports*5 (2016) 395-402,https://doi.org/10.3892/br.2016.747.

[14]N.E. Kushlinskii, M.V. Fridman, E.A. Braga, Molecular Mechanisms and microRNAs in Osteosarcoma Pathogenesis. *Biochemistry* 81 (2016)315-328,https://doi.org/10.1134/S0006297916040027.

[15] A. Rosati, V. Graziano, V. De Laurenzi, M. Pascale, M.C. Turco, BAG3: a multifaceted protein that regulates major cell pathways. *Cell Death and Disease*2 (2011) e141,https://doi.org/10.1038/cddis.2011.24.

[16]Z.-X. Wang, J.-S. Yang, X. Pan, J.-R. Wang, J. Li, Y.-M. Yin, W. De, Functional and biological analysis of Bcl-xL expression in human osteosarcoma. *Bone*47 (2010) 445-454,https://doi.org/10.1016/j.bone.2010.05.027.

[17]J.Li, Z. Yang, Y. Li, J. Xia, D. Li, H. Li, M. Ren, Y. Liao, S. Yu, Y. Chen, Y. Yang, Y. Zhang, Cell apoptosis, autophagy and necroptosis in osteosarcoma treatment.*Oncotarget.*7 (2016) 44763-44778,https://doi.org/10.18632/oncotarget.8206.

[18]C.A.S. Regino, S.V. Torti, R. Ma, G.P.A. Yap, K.A. Kreisel, F.M. Torti, R.P. Planalp, M.W. Brechbiel, *N*-Picolyl Derivatives of Kemp's Triamine as Potential Antitumor Agents: A Preliminary Investigation. *J Med Chem.* 48 (2005) 7993-7999, https://doi.org/10.1021/jm050724r

[19]N. Busschaert, M. Wenzel, M.E., P. Iglesias-Hernández, R. Pérez-Tomás, P.A. Gale, Structure-Activity Relationships in Tripodal Transmembrane Anion Transporters: The Effect of Fluorination. *J Am Chem Soc.* 133 (2011) 14136-14148, https://doi.org/10.1021/ja205884y.

[20] R. Kumar, S. Obrai, A.K. Jassal, M.S. Hundal, J. Mitra, S. Sharma, Synthesis, structure, computational, antimicrobial and *in vitro* anticancer studies of copper(II) complexes with N,N,N′,N′-tetrakis(2-hydroxyethyl)ethylenediamine and tris(2-hydroxyethyl)amine. *J Coord Chem.* 68 (2015) 2130-2146, https://doi.org/10.1080/00958972.2015.1031120

[21] B.G. Gafford, R.A. Holwerda, Oxidative synthesis of bis(.mu.-hydroxo)chromium(III) dimers with aromatic amine ligands. Structure, physical properties, and base hydrolysis kinetics of the bis(.mu.-hydroxo)bis[(tris(2-pyridylmethyl)amine)chromium(III)] ion. *Inorg Chem.*28 (1989) 60-66,https://doi.org/10.1021/ic00300a014

[22]Z. Tyeklár, R.R. Jacobson, N. Wei, N.N. Murthy, J. Zubieta, K.D. Karkin, Reversible reaction of dioxygen (and carbon monoxide) with a copper(I) complex. X-ray structures of relevant mononuclear Cu(I) precursor adducts and the trans-(.mu.-1,2-peroxo)dicopper(II) product. *J Am Chem Soc.* 115 (1993) 2677-2689, https://doi.org/10.1021/ja00060a017

[23] A.F.M. Silva, M.V.P. Mello, J.G. Gómez, G.B. Ferreira, M. Lanznaster, Investigation of Cobalt(III)-Tetrachlorocatechol Complexes as Models for Catechol-Based Anticancer Prodrugs. *Eur J Inorg Chem.* 13 (2019) 1784-1791, https://doi.org/10.1002/ejic.201801550.

[24] H. Nagao, N. Komeda, M. Mukaida, M. Suzuki, K. Tanaka, Structural and Electrochemical Comparison of Copper(II) Complexes with Tripodal Ligands. *Inorg Chem.*35 (1996) 6809-6815,https://doi.org/10.1021/ic960303n

[25]I.M. Wasser, C.F. Martens, C.N. Verani, E. Rentschler, H.-W. Huang, P. Moenne-Loccoz, L.N. Zakharoy, A.L. Rheingold, K.D. Karlin. Synthesis and Spectroscopy of μ-Oxo (O2-)-Bridged Heme/Non-heme Diiron Complexes: Models for the Active Site of Nitric Oxide Reductase. *Inorg Chem.*43 (2004) 651-662, https://doi.org/10.1021/ic0348143

[26]G.J.P. Britovsek, J. England, A.J.P. White, Non-heme iron(II) complexes containing tripodal tetradentate nitrogen ligands and their application in alkane oxidation catalysis. *Inorg. Chem.* 44(2005) 8125-8134, https://doi.org/10.1021/ic0509229

[27] S.S. Massoud, R.R. Jeanbatiste, T.M. Nguyen, F.R. Louka, A.A. Gallo, Cobalt(III) complexes of tripod amines. Kinetics of aquation of dichloro[*N* -(2-aminoethyl)- *N* , *N* - *bis* - (3-aminopropyl)amine]cobalt(III) ion. *J Coord Chem.* 60 (2007) 2409-2419, https://doi.org/10.1080/00958970701271849

[28] A. Beni, A. Dei, S. Laschi, M. Rizzitano, L. Sorace, Tuning the Charge Distribution and Photoswitchable Properties of Cobalt–Dioxolene Complexes by Using Molecular Techniques. *Chem. Eur. J.* 14 (2008) 1804-1813, https://doi.org/10.1002/chem.200701163

[29] M.V. Palmeira-Mello, A.B. Caballero, J.M. Ribeiro, E.M. Souza-Fagundes, P. Gamez, M. lanznaster. Evaluation of cobalt(III) complexes as potential hypoxia-responsive carriers of esculetin. *J. Inorg. Biochem.* 211 (2020) 111211. https://doi.org/10.1016/j.jinorgbio.2020.111211.

[30]A.G. Blackman. The Coordination Chemistry of Tripodal Tetraamine Ligands. *Polyhedron.*24 (2005) 1-39,https://doi.org/10.1016/j.poly.2004.10.012.

[31]T.Mosmann, *J. Immunol. Methods*65 (1983) 55-63, https://doi.org/10.1016/0022-1759(83)90303-4.

[32]A. Doménech-Carbó, A. Maciuk, B. Figadère, E. Poupon, G. Cebrián-Torrejón, Solid-State Electrochemical Assay of Heme-Binding Molecules for Screening of Drugs with Antimalarial Potential. *Anal Chem.* 85 (2013) 4014-4021, https://doi.org/10.1021/ac303746k.

[33] A. Doménech-Carbó, G. Cebrian-Torrejón, L. De Miguel, V. Tordera, D. Rodrigues-Furtado, S. Assad-Kahn, A. Fournet, B. Figadère, R.P.Vázquez-Manrique, E. Poupon, dsDNA, ssDNA, G-quadruplex DNA, and nucleosomal DNA electrochemical screening using canthin-6-one alkaloid-modified electrodes. *Electrochim Acta.*115 (2014) 546-552,https://doi.org/10.1016/j.electacta.2013.11.025.

[34]T.J. Dolinsky, J.E. Nielsen, J.A. McCammon, N.A. Baker, PDB2PQR: an automated pipeline for the setup of Poisson-Boltzmann electrostatics calculations. *Nucleic Acids Res.*1 (2004) W665-W667,https://doi.org/10.1093/nar/gkh381.

[35]T.J. Dolinsky, P. Czodrowski, H. Li, J.E. Nielsen, J.H. Jensen, G. Klebe, N.A. Baker, PDB2PQR: expanding and upgrading automated preparation of

biomolecular structures for molecular simulations. *Nucleic Acids Res.*35 (2007) W522-W252, https://doi.org/10.1093/nar/gkm276.

[36]J. Wang, R.M. Wolf, J.W. Caldwell, P.A. Kollman, Case DA. Development and testing of a general amber force field. *J Comput Chem.*25 (2004) 1157-1174, https://doi.org/10.1002/jcc.20035.

[37]G.M. Morris, R. Huey, W. Lindstrom, M.F. Sanner, R.K. Belew, D.S. Goodsell, A.J. Olson, AutoDock4 and AutoDockTools4: Automated docking with selective receptor flexibility. *J Comput Chem.*30 (2009) 2785-2791,https://doi.org/10.1002/jcc.21256.

[38]J. Gasteiger, M. Marsili, Iterative partial equalization of orbital electronegativity—a rapid access to atomic charges.*Tetrahedron.*36 (1980) 3219-3228,https://doi.org/10.1016/0040-4020(80)80168-2

[39]X. Hou, J. Du, J. Zhang, L. Du, H. Fang, M. Li, How to Improve Docking Accuracy of AutoDock4.2: A Case Study Using Different Electrostatic Potentials. *J Chem Inf Model.*53 (2013) 188-200,https://doi.org/10.1021/ci300417y

[40]G.M. Morris, D.S. Goodsell, R.S. Halliday, R. Huey, W.E. Hart, R.K. Belew, A.J Olson, Automated docking using a Lamarckian genetic algorithm and an empirical binding free energy function. *J Comput Chem.* 19 (1998) 1639-1662,https://doi.org/10.1002/(SICI)1096-987X(19981115)19:14<1639::AID-JCC10>3.0.CO;2-B.

[41]A.C. Wallace, R.A. Laskowski, J.M. Thornton, LIGPLOT: a program to generate schematic diagrams of protein-ligand interactions. *Protein Eng.*8 (1995) 127-134,https://doi.org/10.1093/protein/8.2.127.

[42]R.A. Laskowski, M.B. Swindells, LigPlot+: multiple ligand-protein interaction diagrams for drug discovery. *J Chem Inf Model.* 51 (2011) 2778-2786,https://doi.org/10.1021/ci200227u.

[43]C. Pautke, M. Schieker, T. Tischer, A. Kolk, P. Neth, W. Mutschler, S. Milz. Characterization of osteosarcoma cell lines MG-63, Saos-2 and U-2 OS in comparison to human osteoblasts. *Anticancer Res.*24 (2004) 3743-3748. PMID: 15736406.

[44]H.C.A. Graat, M.A. Witlox, F.H.E. Schagen, G.J.L. Kaspers, M.N. Helder, J. Bras, G.R. Schaap, W.R. Gerritsen, P.I.J.M. Wuisman, V.W. van Beusechem. Different susceptibility of osteosarcoma cell lines and primary cells to treatment with oncolytic adenovirus and doxorubicin or cisplatin. *Br J Cancer*94 (2006)1837–1844.https://doi.org/10.1038/sj.bjc.6603189.

[45] F. Scholz, B. Meyer, in: A.J. Bard, Rubinstein I (Eds.), Electroanalytical Chemistry, New York, 20 (1998) 1.

[46]A. Doménech-Carbó A, Labuda J, Scholz F. Electroanalytical chemistry for the analysis of solids: Characterization and classification. *Pure Appl Chem. 85* (2013) 609-631. https://doi.org/10.1351/PAC-REP-11-11-13

[47]F. Scholz, U. Schröder, R. Gulabowski, A. Doménech-Carbó, Electrochemistry of Immobilized Particles and Droplets, 2ed. Springer, Berlin, 2014.

[48]P. Zuman, C.L. Perrin, Organic Polarography, Wiley, New York, 1969, 275.

[49] A. Doménech-Carbó, G. Cebrian-Torrejón, L. De Miguel, dsDNA, ssDNA, G-quadruplex DNA, and nucleosomal DNA electrochemical screening using canthin-6-one alkaloid-modified electrodes. *Electrochim Acta*. 115 (2014) 546-552, https://doi.org/10.1016/j.electacta.2013.11.025.

[50] S.I. Farooqi, N. Arshad, F. Perveen, P.A. Channar, A. Saeed, A. Javed, T. Hökelek, U. Flörk, Structure and surface analysis of ibuprofen-organotin conjugate: Potential anti-cancer drug candidacy of the compound is proven by in-vitro DNA binding and cytotoxicity studies. *Polyhedron* 192 (2020) 114845. https://doi.org/10.1016/j.poly.2020.114845.

[51] R. Amorim, M.D.F. de Meneses, J.C. Borges, L.C. da Silva Pinheiro, L.A. Caldas, C.C. Cirne, M.V.P. de Mello, A.M.T. de Souza, H.C. Castro, I.C.N. de Palmer Paixão, R.M. Campos, I.E. Bergmann, V. Malirat, A.M.R. Bernardino, M.A. Rebello, D.F. Ferreira, Thieno[2,3-b]pyridine derivatives: A new class of antiviral drugs against Mayaro virus. Arch. Virol. 162 (2017) 1577-1587. http://dx.doi.org/10.1007/s00705-017-3261-0.

[52] C.M. Fernandes, M.V.P. Mello, N.E. dos Santos, A.M.T. de Souza, M. Lanznaster, E.A. Ponzio. Theoretical and experimental studies of a new aniline

derivative corrosion inhibitor for mild steel in acid medium. Materials and Corrosion 71 (2020) 280-291. https://doi.org/10.1002/maco.201911065.

[53]H.R. Drew, R.M. Wing, T. Takano, C. Broka, S. Tanaka, K. Itakura, R.E. Dickerson, Structure of a B-DNA dodecamer: conformation and dynamics. *Proc Natl Acad Sci USA.*78 (1981) 2179-2183, https://doi.org/10.1073/pnas.78.4.2179.

[54]F.A. Hays, A. Teegarden, Z.J.R. Jones, M. Harms, D. Raup, J. Watson, E. Cavaliere, P.S. Ho, How sequence defines structure: A crystallographic map of DNA structure and conformation. *Proc Natl Acad Sci USA*. 102 (2005) 7157-7162,https://doi.org/10.1073/pnas.0409455102.

[55]M.D. Shortridge, M.J. Walker, T. Pavelitz, Y. Chen, W. Yang, G. Varani, A Macrocyclic Peptide Ligand Binds the Oncogenic MicroRNA-21 Precursor and Suppresses Dicer Processing. *ACS Chem Biol.*12 (2017) 1611-1620,https://doi.org/10.1021/acschembio.7b00180.

[56] A. Arakawa, N. Handa, N. Ohsawa, M. Shida, T. Kigawa, F. Hayashi, M. Shirouzu, S. Yokoyama, The C-terminal BAG domain of BAG5 induces conformational changes of the Hsp70 nucleotide-binding domain for ADP-ATP exchange. *Structure.*18 (2010) 309-319, https://doi.org/10.1016/j.str.2010.01.004.

[57]M.K. Manion, J.W. O'Neill, C.D. Giedt, K.M. Kim, K.Y. Zhang, D.M. Hockenbery, Bcl-X_L Mutations Suppress Cellular Sensitivity to Antimycin A. *J Biol Chem.* 279 (2004) 2159-2165, https://doi.org/10.1074/jbc.M306021200.

[58]J.-Q. Du, J. Wu, H.-J. Zhang, Y.-H. Zhang, B.-Y. Qiu, F. Wu, Y.-H. Chen, J-Y. Li, F.-J. Nan, J.-P. Ding, J. Li, Isoquinoline-1,3,4-trione derivatives inactivate caspase-3 by generation of reactive oxygen species.*J Biol Chem.*283 (2008) 30205-30215,https://doi.org/10.1074/jbc.M803347200.

[59]R. Huey, G.M. Morris, A.J. Olson, D.S. Goodsell, A semiempirical free energy force field with charge-based desolvation. *J Comp Chem.* 28 (2007) 1145-1152, https://doi.org/10.1002/jcc.20634.

[60] A. Rosati, M. Ammirante, A. Gentilella, A. Basile, M. Festa, M. Pascale, L. Marzullo, M.A. Belisario, A. Tosco, S. Franceschelli, O. Moltedo, G. Pagliuca, R. Lerose, M.C. Turco, Apoptosis inhibition in cancer cells: A novel molecular

pathway that involves BAG3 protein. *Int J Biochem CellBiol*. 39 (2007) 1337-1342, https://doi.org/10.1016/j.biocel.2007.03.007

[61]L. Xiaokai, T. Colvin, J.N. Rauch, D. Acosta-Alvear, M. Kampmann, B. Dunyak, B. Hann, B.T.Aftab, M. Murnane, M. Cho, P. Walter, J.S.Weissman, M.Y.Sherman, J.E.Gestwicki, Validation of the Hsp70–Bag3 Protein–Protein Interaction as a Potential Therapeutic Target in Cancer. *Mol Cancer Ther.* 14 (2015) 642-648,https://doi.org/10.1158/1535-7163.MCT-14-0650.

[62]S. Wang, D. Yang, M. Lippman,Targeting Bcl-2 and Bcl-X_L with nonpeptidic small-molecule antagonists. *Sem Oncol.* 30 (2003) 133-142, https://doi.org/10.1053/j.seminoncol.2003.08.015

[63]C.A. Lipinski, Lead- and drug-like compounds: the rule-of-five revolution. *Drug Discov Today Technol.*1 (2004) 337-341,https://doi.org/10.1016/j.ddtec.2004.11.007.

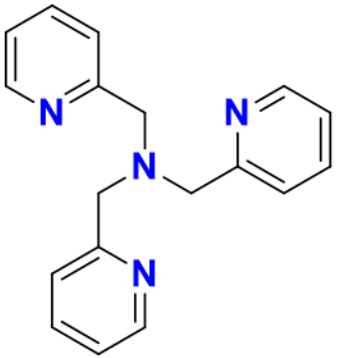

- *Activity against osteosarcoma cells*
- *DNA interaction study*
- *Good pharmacokinetic and toxicological profile*